

# Passive Cylindrical Resonator Temperature Sensor based on Commercial Low-Loss Dielectric Material

Jayaprakash Shivakumar<sup>1</sup>, Nicholas Reed<sup>2</sup>, Cory Clark<sup>3</sup>, Rishikesh Srinivasaraghavan Govindarajan<sup>2</sup>, Daewon Kim<sup>2</sup>, Eduardo Rojas<sup>1</sup>

<sup>1</sup>Department of Electrical Engineering and Computer Science

<sup>2</sup>Department of Aerospace Engineering,

Embry-Riddle Aeronautical University, Daytona Beach, USA

<sup>3</sup>Applications Engineer – WavePro, Palmyra, USA

shivakuj@my.erau.edu, reedn4@my.erau.edu, cory.clark@garlock.com, srinivr1@erau.edu, kimd3c@erau.edu, rojase1@erau.edu

**Abstract**—This research focuses on the development of a passive X-band cylindrical resonator sensor antenna for temperature sensing applications. The resonator sensor antenna design aims to enable precise and real-time monitoring of temperature while embedded inside various materials and structures like polymers and composites. By integrating the sensing capabilities and a slot antenna directly into the cylindrical resonator structure, the research seeks to minimize additional components and streamline the sensing process. The cylindrical resonator sensor antenna operates at a frequency of 10.6 GHz to minimize the size of the resonator and enable high sensitivity and accuracy in detecting subtle changes in temperature. The cylindrical resonator is made from high-permittivity ceramic-loaded PTFE material by WavePro to ensure minimized dielectric losses and allow for sensor miniaturization. The sensor is interrogated through a high bandwidth probing antenna or a Frequency Modulated Continuous Wave (FMCW) radar and the reflected signals are analyzed to extract resonance data. This study proposes a design for the resonator and antenna through high-fidelity simulations and prototypes ensuring reliable and efficient sensing across a range of industrial and structural applications. The outcomes of this research hold the potential to significantly advance the capabilities of temperature monitoring systems. The novelty of this work resides on (a) using a commercial low-loss dielectric material for sensor implementation, (b) the use of advanced manufacturing techniques including 5-axis femtosecond laser machining, and (c) a novel embedded wireless sensor concept. A linear sensor temperature response is measured in the range of 25-210°C, at a sensing distance of 0.5 cm.

**Index Terms**—High Temperature, Sensors, Antennas, Passive, Resonators, Embedded, PTFE, Low-loss, Commercial, RFID, Dielectric.

## I. INTRODUCTION

Additive manufacturing(AM) is transforming sensor development for harsh environments, making it possible to create designs and materials that can handle extreme conditions found in industries like aerospace, automotive, and energy. Additive manufacturing allows for complex shapes that improve sensor performance, resulting in lightweight but durable devices that work reliably in tough conditions. Sensors can be designed with features that integrate multiple sensing capabilities into one passive device. AM facilitates faster prototyping process, allowing quick tests and improvement of

sensor designs based on their performance [1]. The passive resonator-based sensors are used for in-situ measurement of parameters like pressure, strain and temperature using either an interrogating antenna or a wireless Frequency Modulated Continuous Wave (FMCW) Radar. Traditional temperature sensors often fail in harsh conditions due to high heat, corrosive gases, and mechanical stress. Wired sensors can break down, and active sensors typically stop working above 600°C. Passive sensors do not require an external power source; they work by detecting changes in their physical properties to sense physical quantities. This feature makes them ideal for high-temperature settings, as they can endure extreme conditions without failure. These sensors usually detect temperature changes by measuring shifts in resonant frequencies [2], [3]. Real-time in-situ measurement of parameters is important for Structural Health Monitoring (SHM) of critical structures and objects. SHM-based continuous surveillance of structures helps obtain real-time changes in physical parameters and enables preventative maintenance [4]. This is especially necessary for large modular habitats in the extreme environment of space flight where it is not feasible to have bulky wired sensors spread throughout the structure which adds to the size, weight, and power (SWaP) constraints. Furthermore, the sensor needs to be compatible with additive manufacturing process to enable in-space manufacturing and be identified by specific RFID tag [5]. Additionally, with the availability of real-time data, digital twin modeling of structures of critical infrastructure and industrial settings helps in fatigue life estimation with higher accuracy than visual inspection [6]. This paper demonstrates a passive wireless temperature sensor manufactured using ceramic-loaded PTFE, as a precursor to the fully additively manufactured sensor, that is capable of measuring temperature up to 210°C, and interrogated through a waveguide in X-band.

## II. WAVEPRO DIELECTRIC MATERIAL

WavePro dielectrics are ceramic-filled Polytetrafluoroethylene(PTFE) materials made from high-purity PTFE, due to its widely recognized dielectric properties. The dielectric constant can be tuned for any value within a range of 2.5-

20. In addition, the formulations can be modified to enhance specific performance characteristics for special application requirements. During the dielectric manufacturing process, ceramic fillers are added to control various factors, including the dielectric constant, loss tangent, and coefficient of thermal expansion (CTE) of the composite material. Even dispersal of the ceramic fillers within the PTFE host matrix is critical for dielectric performance, material quality, and production yield. The dispersal and mixing involve multiple processing steps to ensure even distribution, prevent agglomeration, and eliminate air pockets and voids. Using a proprietary method, the mixture is initially formed into panels or shapes before being heated above the PTFE melting point of 342°C. The dielectric constant of each slab is verified before proceeding with additional processing steps. The dielectric material used for the sensor in this paper has the following properties as in Table I.

TABLE I  
DIELECTRIC PROPERTIES OF THE SENSOR

Property	Value	Description
D <sub>k</sub>	10.8	Dielectric constant
D <sub>f</sub>	0.0015	Dielectric Loss Tangent
Flammability	V-0	(UL 94 Standard, can be considered self-extinguishing)
Thermal Coefficient of D <sub>k</sub> (TCD <sub>k</sub> )	-327 ppm/°C	0.71 D <sub>k</sub> change from -50°C to 150°C [Fig. 1]
Coefficient of Thermal Expansion (CTE)	X: 22, Y: 19, Z: 21	Z is the thickness of the Dielectric substrate
Density	2.89	grams per cubic centimeter (g/cm <sup>3</sup> )

#### A. Dielectric Material Test Data

The dielectric is tested according to IPC-TM-650-2.5.5.5 standards at around 2.5 GHz and 5 GHz by the manufacturer (Table II). The material's permittivity exhibits a highly linear dependency on temperature, making it a promising candidate for temperature sensors. Between 25°C and 150°C, the permittivity is reduced by 3.4% at a rate of -0.0029/°C.

TABLE II  
MATERIAL TEST DATA: TEST 32044

D <sub>k</sub>	D <sub>f</sub>	Frequency(GHz)
10.73242	0.001259	2.512425
10.76533	0.001219	2.505875
10.73990	0.001238	2.507938
10.75625	0.001404	5.018201
10.79115	0.001393	5.005750
10.76726	0.001373	5.009500

### III. CYLINDRICAL RESONATOR SENSOR DESIGN

The cylindrical resonator is made from a high permittivity WavePro dielectric material to achieve high-quality factor resonance at the design frequencies. Ideally, a material with permittivity greater than 30 times its surroundings would provide high-Q resonance [7]. However, ceramic-loaded PTFE with a permittivity of Er=10.8 was considered for this design. The cylinder is metallized to contain the resonance inside the cylinder and reduce the rate of energy loss [7]. This structure acts as a circular cavity resonator with the dielectric filling the

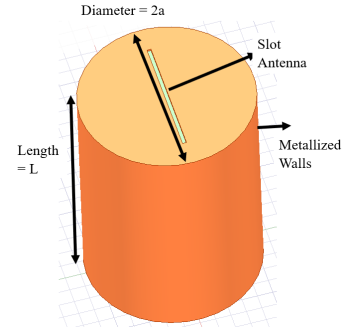


Fig. 1. Geometry of the cylindrical resonator and its slot antenna.

cavity. The dominant resonance mode for this structure is the TE111 where the highest Q-factor is achieved.

#### A. Slot Antenna Design

The slot antenna is designed for the frequency of 10.6 GHz and optimized to match the resonance of the cylinder. The sensor length and the radius are optimized by performing optimetrics sweep in Ansys high-frequency structure simulator (HFSS) to find the desired resonance frequency for different radius and length. Final design values are shown in Table III.

TABLE III  
DIMENSIONS OF CYLINDRICAL RESONATOR SLOT ANTENNA SENSOR

Name	Value	Unit	Description
r <sub>res</sub>	3.5	mm	radius of the resonator
L <sub>res</sub>	10	mm	length of the resonator
t	0.025	mm	thickness of the metal layer
f <sub>o</sub>	10.6	GHz	resonant frequency
λ	(3 × 10 <sup>8</sup> / f <sub>o</sub> )	mm	wavelength
xpos	3	mm	slot distance from the center
L <sub>s</sub>	6.02	mm	length of the slot
W <sub>s</sub>	0.149	mm	width of the slot

The slot antenna is laser machined onto the flat surface of the cylindrical resonator. The slot is etched only on the metallic layer without disturbing the dielectric.

#### B. Prototype Manufacturing

The prototype sensor is manufactured by machining cylinder of dimension 7 mm diameter and 10 mm length out of WavePro dielectric material. The sensor dimension was designed such that the primary resonance occurs at 10.6 GHz. The cylindrical resonator was metallized by screen printing Dupont CB028 silver ink and curing it at 100°C for 90 min to remove the binder and increase the conductivity of the ink. A half wavelength slot antenna is laser machined onto the face of the metallized cylinder using a Spark Lasers DIADEM 1064-10 compact high-energy femtosecond laser with a Thorlabs LMH-20X-1064 high-power focusing 20x objective on a n-Script 3Dn 5-axis tabletop system. The laser machining process uses a peak power of 1 MW, laser path speed of 20 mm/s, repetition rate of 10 kHz, and total number of 20 passes. The femtosecond laser creates pulses of energy for extremely short duration. It is capable of delivering several MW of power for very short duration of femtoseconds which ablates the material with minimal heat affected area around the target area. Thus it

is suitable for micromachining and structuring. The prototype is shown in Fig. 2.

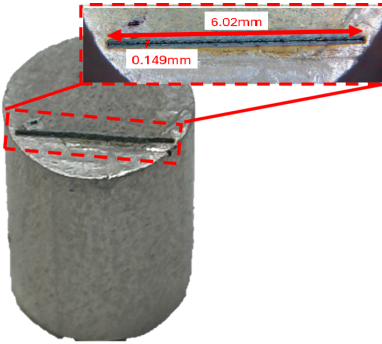


Fig. 2. Manufactured Prototype Resonator Sensor

#### IV. SIMULATION AND MEASUREMENT RESULTS

The Cylindrical Resonator Slot Antenna Sensor is simulated in Ansys HFSS. Ansys HFSS is a 3D electromagnetic (EM) simulation software for designing and simulating high-frequency electronic products such as antennas, antenna arrays, RF or microwave components, high-speed interconnects, filters, connectors, IC packages and printed circuit boards. A frequency domain analysis is performed with a Radiation boundary setup and WR-90 Rectangular Waveguide as the probing device. The simulation setup is shown in Fig. ???. The prototype measurement setup is shown in Fig. 3. The WR-90 waveguide to coaxial adapter is connected to the Keysight N5227B PNA Network Analyzer and the prototype sensor is placed on the hot plate for temperature control. The S-parameters of the Waveguide are recorded in the PNA. Additionally, a FLIR T1020 thermal camera and handheld InfraRed thermometer were setup to measure the temperature of the sensor independently. The thermal image of the sensor at Room temperature is shown in Fig. 4. Using this thermal camera image capture setup, the temperature of the sensor can be remotely monitored without the need for a wired thermocouple on the resonator sensor.

The HFSS simulation shows the presence of strong E fields on the cylinder surface at the slot location indicating a coupling between the resonator and the slot antenna. Additionally, the resonance of the cylinder can be seen by the presence of E-fields in the center of the cylinder. The presence of strong E-fields at the center and J-field at the slot indicates that the slot antenna is coupling the energy from the interrogator waveguide to the resonator and vice versa, and that the sensor is indeed resonating. In Fig. 5, the waveguide clearly registers a reflection from the resonator slot antenna. The  $S_{11}$  for the waveguide in the presence of the resonator is different than in the absent case. The reflection of the sensor can be identified by transforming the  $S_{11}$  to time-domain using the Copper Mountain Technologies RVNA software [2]. Additionally, the resonance of the sensor can be isolated from the  $S_{11}$  by time gating between 22 ns and 40 ns. Time gating is a technique to isolate specific portions of a signal over a defined time

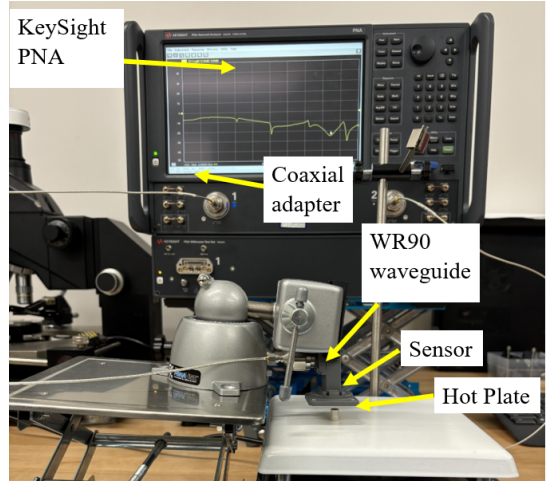


Fig. 3. Measurement Setup: PNA, WaveGuide, Hot Plate, Sensor

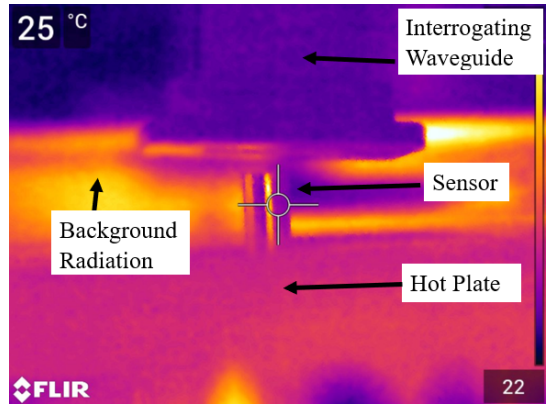


Fig. 4. Thermal Camera Image at Room Temperature

window. Time gating helps isolate reflections from specific devices, in this case, the sensor. By applying time gating, the resonance reflection from the sensor can be isolated from the waveguide  $S_{11}$  which is a composite of waveguide ringing, impedance mismatch and material losses, coupling effects, and the sensor resonance reflection. The sensor resonant frequency can then be extracted by transforming back to the frequency domain as shown in Fig. 6. The peak resonance frequency at room temperature was extracted as 10.45 GHz. This is different from the designed resonance frequency of 10.6 GHz due to limitations in the manufacturing accuracy of the sensor in our prototype lab and small variations in the material properties. As a temperature sensor, the peak resonance frequency shifts with an increase in the temperature. When the sensor is embedded inside a structure and the temperature changes, the temperature of the sensor also changes due to the good thermal conductivity of the sensor material. The temperature of the structure can thus be estimated.

Fig. 7 shows the resonance of the sensor at different temperatures ranging from 25°C to 210°C. The resonance peak is different for each case and can be distinguished by a computer algorithm to find the corresponding temperature.

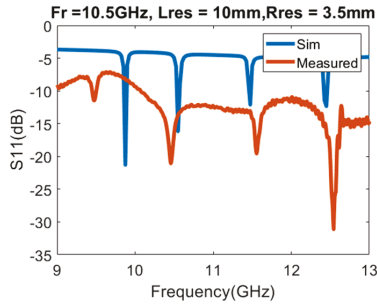


Fig. 5. Sensor Simulation and Measured results

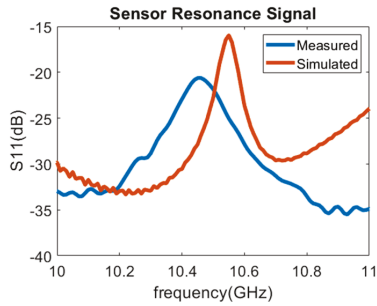


Fig. 6. Resonance of the sensor

An important source of error in the measurement is induced due to the presence of a temperature gradient along the height of the sensor cylinder. This was overcome by measuring the sensor temperature after temperature throughout the sensor had stabilized and when gradient was minimal. In Fig. 8, the resonant frequency is plotted against the temperature in 10°C steps. The linear approximation equation can be used to interpolate the temperature for intermediate temperatures. With a more accurate sensor temperature measurement setup and lower intermediate frequency in the PNA, the sensor temperature resolution can be further improved to 5°C steps.

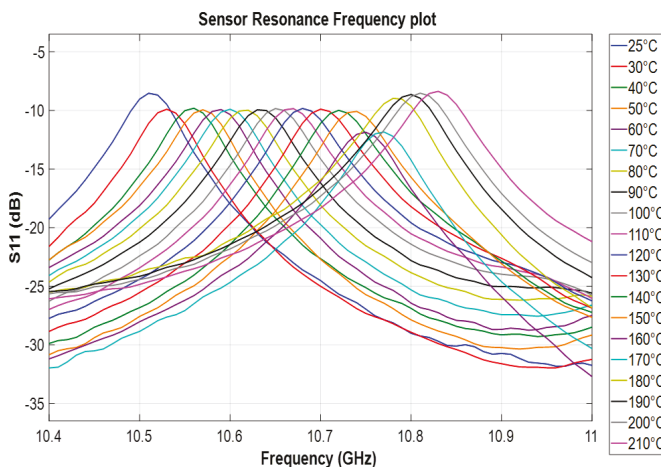


Fig. 7. Temperature shift of the Sensor Resonance

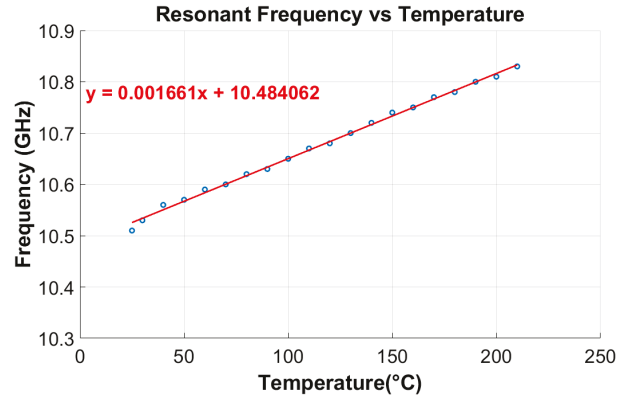


Fig. 8. Temperature and Resonance Frequency relationship

#### ACKNOWLEDGMENT

This material is based upon work supported by the National Science Foundation under Grant No.2229155 and 1944599. The opinions, findings, and conclusions, or recommendations expressed are those of the authors and do not necessarily reflect the views of the National Science Foundation. Thanks to WavePro for providing material and engineering support for this work.

#### REFERENCES

- [1] Seng Loong Yu, Swadipta Roy, Sreekala Suseela, Taofeek Orekan, Joshua McConkey, Reamonn Soto, Eduardo A. Rojas-Nastrucci, "Advanced Manufacturing of Passive Wireless High-Temperature Pressure Sensor Using 3-D Laser Machining", IEEE 22nd Annual Wireless and Microwave Technology Conference (WAMICON), Clearwater, Florida, USA, 27-28 April 2022.
- [2] Haitao Cheng, Xinhua Ren, Siamak Ebadi, Yaohan Chen, Linan An, and Xun Gong, "Wireless Passive Temperature Sensors Using Integrated Cylindrical Resonator/Antenna for Harsh-Environment Applications" IEEE SENSORS JOURNAL, vol. 15, pp. 1453–1462, March 2015.
- [3] Maria V. De Paolis, Julien Philippe, Alexandre Rumeau, Anthony Couscou, Samuel Charlot, Hervé Aubert, and Patrick Pons, "APERTURE-COUPLED MICROSTRIP RESONATOR FOR MILLIMETER-WAVE PASSIVE PRESSURE SENSORS", Transducers 2019 - EUROSENSORS XXXIII, Berlin, GERMANY, 23-27 June 2019.
- [4] JUN WANG, TIANTIAN WANG, AND QIZHANG LUO, "A Practical Structural Health Monitoring System for High-Speed Train Car-Body", IEEE Access, vol. 7, 2019.
- [5] Carlos R. Mejias-Morillo, Audrey Gbaguidi†, Dae Won Kim, Sirish Namilae, Eduardo A. Rojas-Nastrucci, "UHF RFID-based Additively Manufactured Passive Wireless Sensor for Detecting Micrometeoroid and Orbital Debris Impacts", IEEE International Conference on Wireless for Space and Extreme Environments (WiSEE), Ottawa, Canada, 16-18 October 2019.
- [6] Chungkuk Jin; Sung-Jae Kim; MooHyun Kim; Amitava Guha; Dong-hwan Lee; Oleg E. Esenkov; Wei Xu; Benjamin Smith; Sam Ryu, "Digital Twin Method for Global Motion and Stress Monitoring of a Steel Lazy Wave Riser", OCEANS 2022, Hampton Roads, Hampton Roads, VA, USA, 2022, pp. 1-7, doi: 10.1109/OCEANS47191.2022.9977010.
- [7] Constantine A. Balanis, "ADVANCED ENGINEERING ELECTROMAGNETICS", SECOND EDITION, pp 352–548, April 2012.
- [8] Thomas M. Weller, Linda P. B. Katehi, and Gabriel M. Rebeiz, "Single and Double Folded-Slot Antennas on Semi-Infinite Substrates", IEEE TRANSACTIONS ON ANTENNAS AND PROPAGATION, VOL. 43, NO. 12, DECEMBER 1995.